Marine Science Center-University of Basrah

Mesopotamian Journal of Marine Sciences
Print ISSN: 2073-6428
E- ISSN: 2708-6097
www.mjms.uobasrah.edu.iq/index.php/mms

Impact of a Proposed Barrage on the Tidal Wave Characteristics and Salinity Distribution in the Shatt Al-Arab River Estuary

iD Ali A. Lafta and iD Sadiq S. Abdullah
Marine Science Center - University of Basrah, Iraq
**Corresponding Author: e-mail: ali.lafta@uobasrah.edu.iq*

Article info.
- ✓ *Received: 10 May 2024*
- ✓ *Accepted: 27 June 2024*
- ✓ *Published: 29 June2024*

Key Words:
Harmonic analysis,
Mike11,
Salinity intrusion,
Shatt Al-Arab river.
Tidal wave

Abstract - The response of the tidal hydrodynamics and salinity status in the Shatt Al-Arab river estuary (SARE) to the installation of a barrage was investigated using Mike11. The results demonstrated that installing a barrage might cause many changes in the hydrodynamic behavior of SARE. The most noticeable alteration occurs in the tidal range, particularly near the barrage location, where there are significant increases in the tidal range in such regions. However, tidal range variations are intimately correlated with tidal constituents amplitude variations, particularly in the vicinity of the barrage site, where the largest amplitude variation of the tidal components occurs. To examine the variations in the tidal constituent characteristics, six stations were chosen. In the first three stations, there was a significant increase in the amplitudes of the semi-diurnal components, namely M2, S2, and N2, whereas in the other stations, there was a slight decrease. Conversely, the diurnal constituents amplitudes exhibit a notable increase in the first five stations but remain unchanged in the sixth. Furthermore, there are noticeable variations in the phase of the tidal components, with the most significant change occurring between stations five and six. Additionally, several scenarios were performed to determine the appropriate freshwater inflow from the Karun river to maintain the SARE environment. Based on the results, it appears that freshwater flows of 70, 80, 90, and 100 m3/sec may be suitable to sustain the SARE environment, as long as the length of the salinity incursion remains below 60 km.

تأثير السدة المقترح انشاؤها على خصائص الموجة المدية وتوزيع الملوحة في مصب شط العرب ، جنوب العراق

علي عبد الرضا لفته و صادق سالم عبدالله
مركز علوم البحار- جامعة البصرة – البصرة - العراق

المستخلص - تم دراسة تأثير السدة التنظيمية المقترحة على هيدروديناميكا المد والجزر وحالة الملوحة في مصب شط العرب باستخدام حزمة بيانات Mike11. أظهرت النتائج أن انشاء السدة التنظيمية قد يسبب العديد من التغييرات في السلوك الهيدروديناميكي للنهر. يحدث التغيير الأكثر وضوحًا في مدى المد والجزر، خاصة بالقرب من موقع السدة، حيث توجد زيادات كبيرة في مدى المد والجزر في هذه المناطق. ترتبط اختلافات مدى المد والجزر ارتباطًا وثيقًا بتغيرات سعة مقومات المد والجزر، خاصة في المنطقة المجاورة لموقع السدة، اذ يحدث أكبر اختلاف في سعة مقومات المد والجزر. تم اختيار ست محطات لدراسة التغيرات في خصائص الموجة المدية، اذ وجد ان هناك زيادة كبيرة في سعات المقومات المدية نصف اليومية في المحطات الثلاث الأولى وهيM2 ، S2، وN2، بينما في المحطات الأخرى، كان هناك انخفاض طفيف في سعات هذه المقومات المدية. على العكس من ذلك، اظهرت سعة المقومات المدية اليومية زيادة ملحوظة في المحطات الخمس الأولى ولكنها تظل دون تغيير في المحطة السادسة. علاوة على ذلك، وجد ان هناك اختلافات ملحوظة في اطوار مقومات المد والجزر، حيث يحدث التغيير الأكثر أهمية بين المحطتين الخامسة والسادسة.. بالإضافة إلى ذلك، تم تنفيذ عدة سيناريوهات لتحديد تدفق المياه العذبة المناسب من نهر الكارون للحفاظ على بيئة شط العرب. وبناء على النتائج، تبين أن تصريف المياه العذبة من نهر الكارون بمقدار 70، 80، 90، 100 م^3/ثانية قد تكون مناسبة للحفاظ على بيئة شط العرب من توغل الاملاح باتجاه اعالي مصب شط العرب.

كلمات مفتاحية: الموجة المدية، التحليل التوافقي، توغل الاملاح، مايك 11، شط العرب.

Introduction

One of the most common issues in estuarine systems is salinity intrusion, which has a variety of negative impacts on the local economy, ecology, and society. Numerous sources, both natural and man-made, may have an impact on this particular issue. The construction of upper river dams, which reduces the amount of freshwater reaching the lower part of a tidal river, is one familiar example of an anthropogenic factor. Furthermore, natural impacts might be related to changes in climatic patterns, such as decreased precipitation, rising sea levels, and increased storm surge severity (Haddout and Maslouhi, 2018; Liu *et al.*, 2014; Wachler *et al.*, 2020).

Shatt Al-Arab River is the primary supplier of surface water for several urban areas, including Basrah in Iraq and Khuzestan in Iran (Allafta and Opp, 2020; Lafta, 2022). In addition, the estuary is a key supplier of freshwater for the northern Arabian Gulf and has a vital effect on the Gulf's marine environment (Al-Yamani, 2008). With millions of palm trees lining its banks, the SARE area was once regarded as a highly productive region. Nevertheless, the Shatt Al-Arab river has encountered numerous issues over the past two decades, which have clearly worsened the quality and quantity of its water (Abdullah, 2016; Moyel and Hussain, 2015). The Tigris, Euphrates, and Karun rivers were continuously dammed and controlled in Turkey, Syria, Iran, and Iraq, which reduced the amount of freshwater entering the SARE system. As a result, sea water from the Arabian Gulf pushed further upstream into the river's upper sections. So, this issue became familiar during the dry months and more frequent in the last years. Those living nearby protested, and there were numerous financial damages in the city as a result. Numerous solutions are suggested in order to address this issue and stop the saline infiltration into Basrah city (Mahmood *et al.*, 2022). The construction of a barrage along the SARE stream flow was one among these suggestions. However, adding any artificial structures to a natural river system may have a number of negative repercussions that must be considered before proceeding. According to Neill *et al.*, (2018), any regulatory establishment could have an enormous effect on the river ecology, and implications should be considered prior to installation. In the Severn Estuary, Qian Ma *et al.*, (2019) investigated the impact of a tidal barrier on storm surge-induced coastal flooding. They showed how the establishment of such a structure might assist in reducing the impact of storm surges on coastal flooding. Fairley *et al*., (2014) investigated the effect of a Severn Barrage on the dynamics of tidal waves across the Bristol Channel and demonstrated that the regulating dam might alter tidal currents and wave amplitude. According to Ali and Al Thamiri, (2021), the construction of a barrage in the Shatt Al-Arab River causes a considerable decrease in flow velocity upstream of the barrage, which increases sedimentation in the river's course and has a detrimental effect on navigation safety. The main aims of the current study are to examine how the installation of a barrage inside the estuary system affects the tidal hydrodynamics and salinity intrusion extent of the SARE system. A numerical model based on the one-dimensional numerical modeling package Mike11 was developed to achieve the study objectives.

Materials and Method

Study Area

Historically, SARE was formed by the merging of the Tigris and Euphrates, and the other tributary is the Karun river. However, the Euphrates river was cut off from the Shatt Al-Arab river by the construction of an embankment, making the Tigris river the main supply of freshwater nowadays. When there is an abundance of water in the Karun River, it might be regarded as a secondary source of freshwater for the SARE.

Shatt Al-Arab river runs for approximately 204 kilometers, starting in Qurna and ending 10 km south of Faw city, where it enters the Arabian Gulf, as illustrated in figure (1). The river's width ranges from roughly 1000 m near the estuary mouth to about 300 m in Qurna city (Lafta, 2021). The deepest area of the river is roughly 20 m (Lafta, 2021). Freshwater discharge, tidal regime, and the prevailing weather all influence the river's hydrology. The estuary tidal regime is mostly influenced by the tidal system of the northwest Arabian Gulf, which is a mixed tide, with mostly semidiurnal (Abdulla, 2002; Lafta *et al*., 2020). The region experiences a hot and long-lasting summer. The region receives little rain on an annual basis, and it mostly falls in the winter months. Two different wind regime types can be found in the area, specifically, the southeast wind and northwest wind (Shamal wind) (Zakaria *et al*., 2013).

(Figure 1) Map of the studied area.

Data Source

The study's objectives required a variety of data, including measurements of salinity, bathymetry, and water level fluctuations. In March 2017 at two places, Sihan and Abo Flous (see figure 1), a pressure water level diver and conductivity diver type Hopo, were installed to record the water level and salinity. The observations of the water levels are made in relation to a local datum known as Faw 1979, which is the mean sea level at Faw City. Using the empirical approach, salinity can be calculated as follows: salinity=0.64*conductivity. The geometry of the SARE model was created by Mike11 using bathymetric and topography observations along the SARE and Tigris river. Both the bathymetric survey conducted by the Ministry of Water Resources through 2012 and the measurements carried out by the Marine Science Center/University of Basrah between 1998 and 2005, were used. Additionally, and as a result of

the Karun river's absence of bathymetric data, the geometry of this river was created using satellite data as well as Google Earth images.

Harmonic Method

The harmonic technique is commonly employed in coastal systems to investigate tidal dynamics and asymmetry (Iglesias *et al.,* 2019; Mao *et al.,* 2004; Siddig *et al.,* 2019; Suh *et al.,* 2014). This approach is depend on computing the amplitudes and phases of the tidal components using tidal data sets (Boon, 2013). In this work, the tidal analysis tool named Matlab world Tides was employed. More information about this approach, how to get it, and how to use it may be available at (https://www.mathworks.com/matlabcentral/fileexchange/24217-world-tides).

Tidal asymmetry can be formed if the two interacting components fulfill $2\omega_1 = \omega_2$ and $\omega_1 + \omega_2 = \omega_3$ (ω is the constituent frequency) (Song *et al.,* 2011).The relative phase relations, most commonly $2\theta_1 - \theta_2$ and $\theta_1 + \theta_2 - \theta_3$ (θ is the constituent phase in degrees), are primarily used to identify the kind of tidal asymmetry. For example, in semi-diurnal tidal estuaries, the interaction of the M2 with its first harmonic M4 was widely regarded as the primary source of tidal asymmetry (Aubrey and Speer, 1985; Friedrichs and Aubrey, 1988). A tidal wave with an ebb dominance is associated with a phase difference ($2\theta_1 = \theta_2$) between 180 and 360 degrees, whereas a phase difference between 0 and 180 degrees indicates a shorter duration of rising tide than falling tide or a flood dominance.

Model Preparation

The study's methodology involves using Mike11 to create the hydrodynamic and transport model. However, Mike11 is a one-dimensional modeling package that employs a finite difference approach to solve Saint-Venant equations. By resolving the Advection-Diffusion equation, the salinity distribution is simulated. In the Mike11 user handbook (DHI, 2007), more information on the model's properties, methodology, and applications is provided.

The model of the SARE consists of one primary stream flow path and three lateral branches. However, the main stream originated from the Tigris river, at a sharing border between Al Basrah and Missan provinces, and it ended at Faw city, which is close to where the SARE and the Arabian Gulf confluence. According to Figure (1), the Euphrates, Karmat Ali, and Karun rivers are represented by the other three branches.

The upstream of the Euphrates river branch is located at the embankment built along its path and extends to about 35 km and finishes at Qurna city when it meets the Tigris river. The Karmatt Ali river branch, meanwhile, stretches for about 18 km from the Al-Hammar marsh to the point where it meets the SARE. However, the Karun river branch extends from Darkhovin region to the location where it joins the SARE for around 50 km (see figure 1). For the Shatt Al-Arab model's upstream boundary condition, the freshwater discharge from the Tigris river was employed, and for the downstream boundary condition, the fluctuations in water levels in Faw City were used (figure 2). For the Karun river, the freshwater discharge at the Darkhovin region was used as an upstream boundary condition.

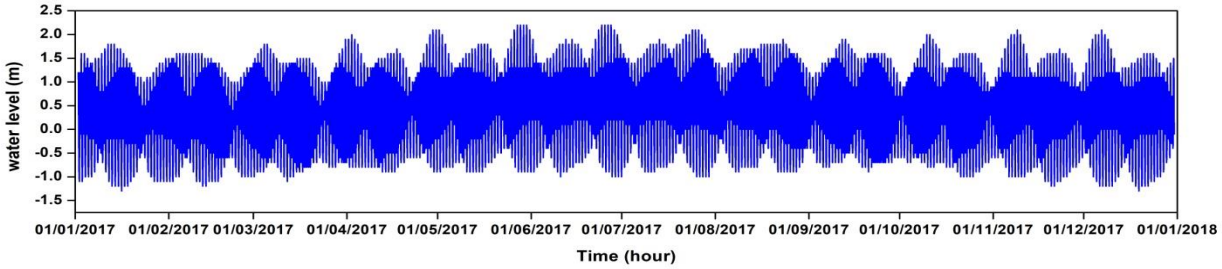

(Figure 2) Water level fluctuation at Faw city.

The primary model path and all of its tributaries were discretized spatially every 250 m. The SARE model was run for entire of year 2017. The model's stability was attained depending on the Courant-Friedrichs criterion by using a time step of 120 seconds. At the downstream boundary, the salinity was assumed 35 ppt, whereas the salinity upstream of the SARE and Karun river was 1 ppt.

The model's performance was assessed through comparing predicted water level and salinity values with observations at two sites, Sihan, and Abo Flous. The root mean square error (RMSE) was used to verify the model's performance.

$$(\mathrm{RMSE} = \sqrt{\frac{\sum_{i=1}^{N}(Mi-Ci)2}{N}}),$$

Where, M_i and Ci are a sum of measured and simulated values respectively, and N is a number of values. The model performed most efficiently when the freshwater inflow of the Tigris and Karun rivers were at 50 and 5 m^3/sec, respectively, with a bottom roughness (manning number) of 0.17 ($m^{1/2}$/sec).

Comparisons of the predicted and observed water levels at the Sihan and Abo Flous sensors with RMSE of 0.13 and 0.06 m, respectively, are shown in Figure (3). The salinity data from the Sihan sensor were utilized for the comparison, and a qualitative match was reached between observed and predicted salinity.

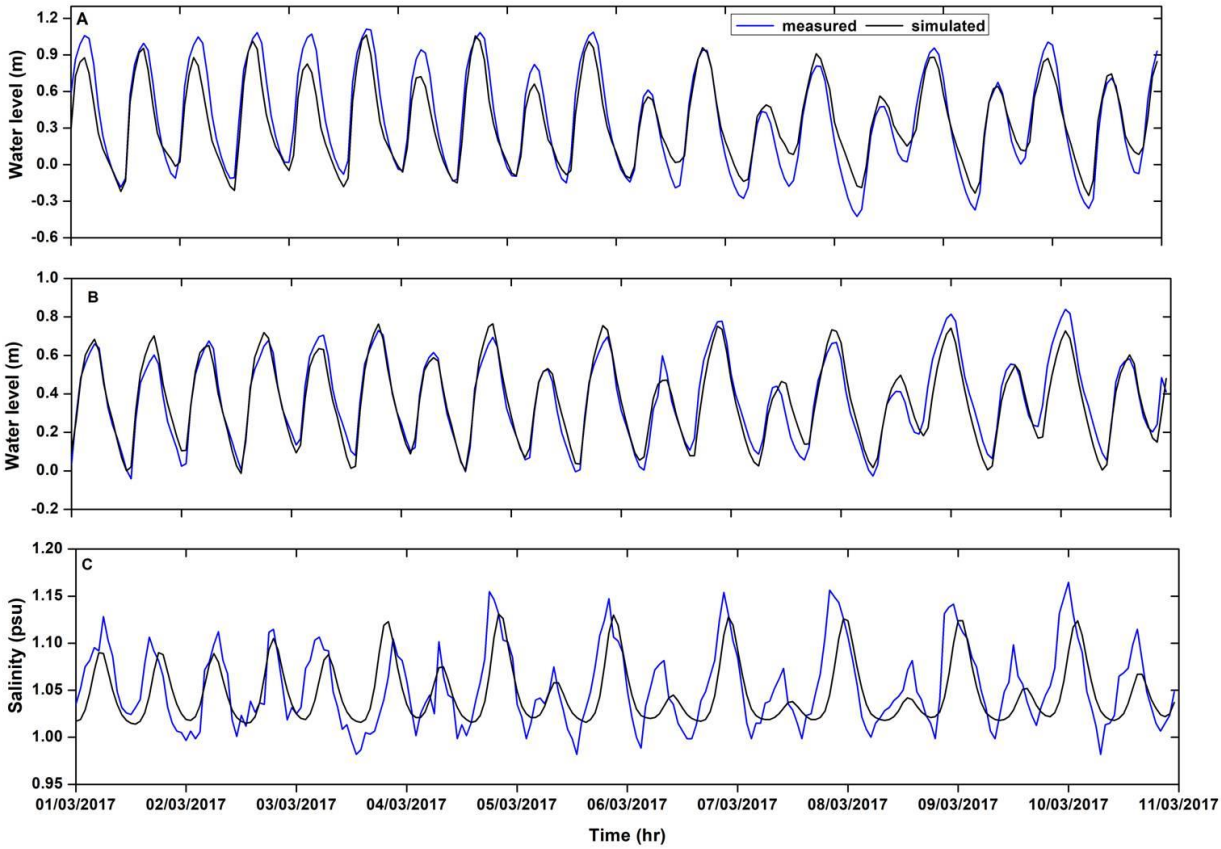

(Figure 3) Comparison of salinity and water level observed data at (A and C: Sinhan, B: Abu Flous) with model results.

Result and Discussion

To evaluate the two scenarios of the tidal characteristics, i.e. before and after the installation of the barrage on the estuary stream, the hydrodynamic model results were examined.

Effect of the Proposed Barrage on Tidal Hydrodynamics

Changes in Amplitude and Phase of Principal Constituents

Generally speaking, the hydrodynamic regime of an estuary will vary in multiple ways when an engineered construction is added to its natural system. The hydrodynamic behavior of the SARE is being compared before and after the installation of a barrage at six different locations along the estuary in order to look into potential alterations in this behavior. Table (1) indicates the distance between each of the selected stations and the site of the barrage. The relative variations in the tidal harmonics of the tidal wave that propagates from the northern Arabian Gulf to the higher reaches of the SARE, however, serve as the basis for the comparison of the tidal hydrodynamics.

(Table 1) The distance between the selected stations and the site of the barrag

.

Station	Distance to Barrage (km)
St 1	1
St 2	10
St 3	24
St 4	44
St 5	63
St 6	80

The response of constituents amplitude to the presence of the barrage in the estuary system was spatially non-uniform, with substantial decreases and increases between different selected stations. Table (2) shows the computed amplitudes and phases of the principal tidal constituents at the selected SARE stations before and after installing the barrage in the estuary system. The principle lunar semidiurnal component, M2, which is the largest tidal component in the SARE (Abdulla, 2002; Lafta, 2022), appears to be changing significantly as the barrage is installed at the estuary system. The M2 amplitude increased significantly in the first three stations (St1, St2, and St3) and decreased slightly in the other stations. The greatest percentage increase occurs in the first station, i.e., directly downstream of the barrage, by about 53% from 0.239 to 0.515 m. As we moved further below the barrage, the increasing amount of M2 amplitude decreased, in St2, for instance, the increasing percentage was 40%, while, in St3 was only 3%. Other stations exhibit an opposite behavior, with a noticeable decline in the amplitude of the M2 constituent. However, the percentage of amplitude decrease was minimal in St4, St5, and St6, with 5%, 3%, and 1%, respectively. Likewise, the S2 response exhibited irregularities, with a significant rise in amplitude in the first three stations located within the study area, and a slight decrease in other stations. In St1, St2, and St3, the increasing S2 amplitude was 52%, 38%, and 1%, respectively. In while, St4, St5, and St6 had decreasing amounts of 4%, 3%, and 1%, respectively. Furthermore, in St1, St2, and St3, the N2 amplitude rises by 52%, 38%, and 2%, respectively. Meanwhile, St4, St5, and St6 all showed a slight decrease in N2 amplitude of 5%, 3%, and 1%,

respectively. However, in contrast to the semidiurnal constituents, the amplitude of the principal diurnal constituents increases noticeably when the barrage is introduced to the estuary system. K1 amplitude shows no considerable change in the St6 and an increase in the other five stations. For each of the following: St1, St2, St3, St4, and St5, the amplitude of K1 increases by 50%, 45%, 22%, 6%, and 1.6%, respectively. While O1 behaved similarly to K1, with no change in St6 and significant increases in the other stations. In St1, St2, St3, St4, and St5, the amplitude of O1 increases by 47%, 43%, 21%, 6%, and 1%, respectively.

(Table 2) Amplitude A (m) and Phase P (degree) of the tidal constituents at SARE

Const.	St 1				St 2				St 3			
	Without Barrage		With Barrage		Without Barrage		With Barrage		Without Barrage		With Barrage	
	A	P	A	P	A	P	A	P	A	P	A	P
O1	0.107	303.09	0.205	286.75	0.115	290.55	0.205	286.41	0.158	259.24	0.202	267.27
K1	0.177	24.49	0.358	10.7	0.193	11.9	0.357	10.3	0.282	340.73	0.362	349.87
N2	0.047	271.22	0.099	270.68	0.059	251.54	0.096	269.75	0.109	212.53	0.111	229.06
M2	0.239	23.08	0.515	25.01	0.301	4.35	0.502	24.52	0.541	327.25	0.559	345.11
S2	0.065	139.92	0.137	140.98	0.083	121.59	0.134	140.31	0.162	84.71	0.164	99.97
M4	0.039	290.74	0.084	286.45	0.05	269.87	0.077	284.82	0.11	239.94	0.101	252.27
Const.	St 4				St 5				St 6			
	Without Barrage		With Barrage		Without Barrage		With Barrage		Without Barrage		With Barrage	
	A	P	A	P	A	P	A	P	A	P	A	P
O1	0.202	241.98	0.215	247.92	0.229	231.76	0.231	234.69	0.243	223.29	0.243	223.84
K1	0.368	324.71	0.393	330.85	0.411	316.26	0.418	319.09	0.433	308.52	0.434	309.04
N2	0.152	192.68	0.144	199.44	0.166	181.37	0.161	184.16	0.167	169.45	0.166	169.8
M2	0.74	307.2	0.702	314.81	0.807	296	0.779	299.1	0.813	284.73	0.806	285.13
S2	0.226	65.73	0.215	72.05	0.247	54.69	0.239	57.2	0.25	42.24	0.248	42.55
M4	0.132	220.1	0.111	225.83	0.096	200.91	0.083	201.46	0.061	160.25	0.059	158.93

The obtained results are more obvious in the estimated tidal range values. The tidal range at St1 increased to 1.636 m when the barrage was put up in the estuary system, up from 0.764 m before the barrage was installed. However, this is not a surprise result and might be attributed to the tidal wave's confinement in the estuary system in a reducing region as the wave propagates further up to the inland direction. This behavior, however, is likely comparable to that of the tidal wave in convergent estuaries when the tidal range rises towards the inland direction (Vinita *et al.*, 2015). However, the tidal range changes decreased as we moved on south of the barrage site, where the changes are low and just a few centimeters in St6. These findings are consistent with

Abdullah *et al.*, (2023) prior conclusion that installing a barrage could change the tidal range in SARE, particularly near the barrage location.

Table (3) displays the tidal phase response of the principal tidal constituents to the planned tidal barrage. However, due to the nature of tidal wave propagation at shallow water bodies, the reduction in tidal constituents' phases suggests that tidal waves will arrive earlier. The constituent phase shift describes the time of tidal arrival T, which may be calculated using (Kuang *et al.*, 2016):

$$T = \frac{\Delta g}{360} \times T_{const.}$$

where Δg is the phase change and $T_{const.}$ is the tidal constituent period. The phase change between St6 and St1 for the M2 component (T_{M2}=12.42 h) was roughly 99 degrees, i.e., 204 minutes, implying that the crest of the tidal wave took 3.4 hours to travel from St6 to St1. The installation of the barrage raises the phase change of M2 to 100 degrees, requiring the tidal wave to arrive at St1 in approximately 207 minutes. In practice, this adjustment seemed to be ineffective, but the startling results were the phase changes between the stations themselves. The phase difference between the two states is seen in Table (3). When the barrage is put into the estuary system, the M2 largest phase shifts occur between St2 and St1 and reach roughly 18 degrees, causing the tidal wave to propagate 37 minutes faster between these two places. Similarly, the phase difference of both N2 (T_{N2}=12.69 h) and S2 (T_{S2}=12 h) behaviors are comparable to that of M2, with not any significant variations in the phase difference between St1 and St6 observed between the two states. The most significant alterations occur between St1 and St2, with the phase change occurring at around 19 and 18 degrees for N2 and S2, respectively (table 3). Additionally, there are no significant variations in the phase difference between St1 to St6 between the two states for the diurnal components K1 and O1, while there are significant variations between St1 and St2. For both K1 (T_{K1}=23.93 h) and O1 (T_{O1}=25.81 h), the phase difference between the St1 and St2 will decrease by roughly 12 degrees, respectively. Therefore, it is possible for these tidal elements to leave St2 and arrive at St1 approximately 48 minutes earlier.

(Table 3) The constituents phase changes (degrees) at the selected stations along the SARE

Const.	Barrage state	Stations	Stations	Stations	Stations	Stations
		St2, St1	St3, St2	St4, St3	St5,St4	St6, St5
M2	Without Barrage	18.73	37.1	20.05	11.2	11.27
	With Barrage	0.49	39.41	30.3	15.71	13.97
S2	Without Barrage	18.33	36.88	18.98	11.04	12.45
	With Barrage	0.67	40.34	27.92	14.85	14.65
N2	Without Barrage	19.68	39.01	19.85	11.31	11.92
	With Barrage	0.93	40.69	29.62	15.28	14.36
O1	Without Barrage	12.54	31.31	17.26	10.22	8.47
	With Barrage	0.34	19.14	19.35	13.23	10.85
K1	Without Barrage	12.59	31.17	16.02	8.45	7.74
	With Barrage	0.4	20.43	19.02	11.76	10.05

Effect of the Proposed Barrage on Tidal Asymmetry

Tidal asymmetry can be produced by combining two or more astronomical or mixed astronomical and shallow water components (Guo *et al.*, 2019; Provost, 1991; Song *et al.*, 2011).

The relative phase relation between M2 and M4 ($2\theta_{M_2}$-θ_{M_4}) were 115, 98, 54, 34, 31.09, and 49 degrees at St1, St2, St3, St4, St5, and St6, respectively. Therefore, SARE displays a flood dominance tendency, according to Aubrey and Speer (1985). The M4/M2 amplitude ratio higher than 0.01 implies considerable tidal distortion in the tidal system, as reported by Lu *et al*., (2015). In SARE, this value varied from 0.07 to 0.2 and demonstrated an irregular evolution trend, growing from St6 to St3, and then decreasing to the remaining stations. The progression of this ratio, however, is dependent on the dynamics of the two components M2 and M4. When this ratio rises, it indicates a significant energy transfer from M2 to M4, and its spatial distribution is strongly influenced by the local geometry of the estuary. However, when a proposed barrage is added to the estuary system, the relative phase between M2 and M4 rises to 123, 124, 77, 43, 36, and 51 degrees in St1, St2, St3, St4, St5, and St6, respectively. As a result, and based on the findings of Aubery and Speer (1985), the relative phase relation remains less than 180 degrees, and the tidal asymmetry in SARE remains flood-dominant.

Effect of the Proposed Barrage on Salinity Intrusion

Salinity intrusion length is used to describe the movement of saline water from the sea farther into the upper reaches of estuaries when freshwater inflow is reduced in estuarine systems. According to Parsa *et al.*, (2007) and Shivaprasad *et al.*, (2013), the length of salinity intrusion is the distance from the estuary mouth to a point where the salinity is higher than the riverine water by 1 ppt. Several numerical simulations were carried out to determine the most popular freshwater inflow from the Karun river to preserve the SARE ecosystem from salinity intrusion when the river is blocked by the barrage.

The first scenario is based on the most extreme state that assumed the entirely cut-off of freshwater inflow from the Karun River (freshwater inflow=0 m^3/sec). The findings of this scenario suggested that the salt intrusion length at the end of the simulation approaches the position of the barrage, and that the whole area located behind the barrage could turn into entirely saline water region (figure 4). The saline water takes around 20 days to reach the barrage location. For the Karun river, saline water will travel towards upstream to the Darkhovin region, which will take around five months (figure 5).

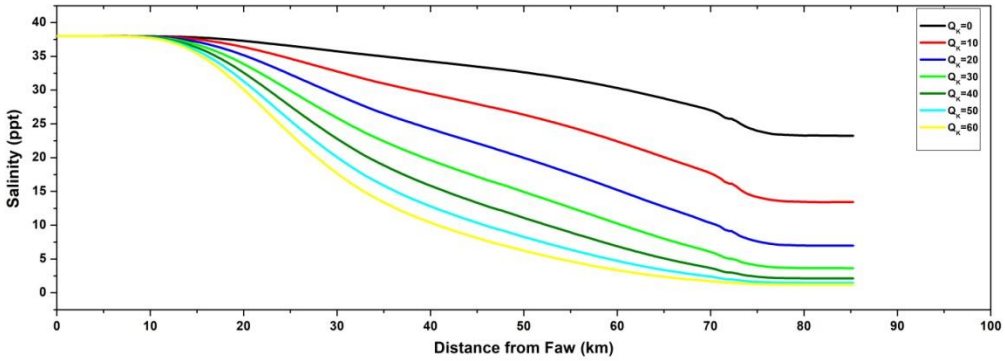

(Figure 4) Salinity intrusion length (km) along SARE corresponding to several freshwater inflow (0- 60 m3/sec) from Karun River

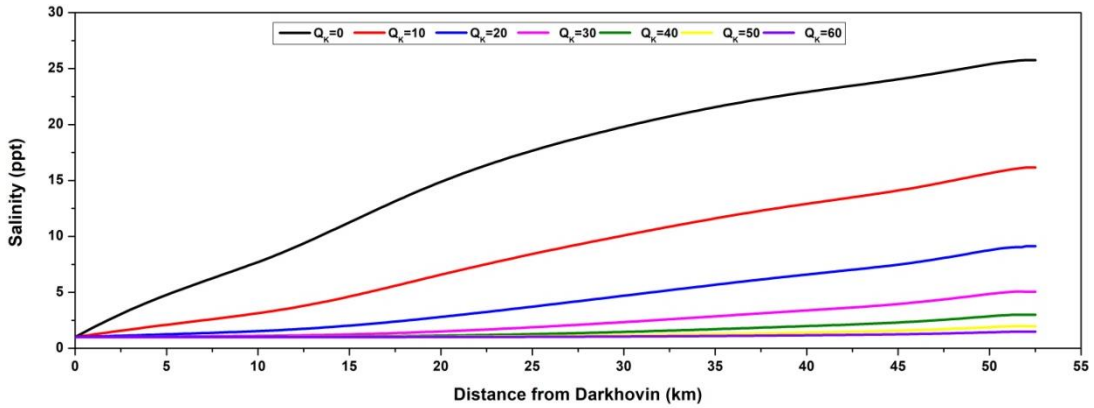

(Figure 5) Salinity intrusion length (km) along Karun river corresponding to several freshwater inflows from Karun River.

The second scenario is based on a Karun freshwater inflow of 10 m^3/sec. According to scenario results, saline water takes approximately 25 days to reach the barrage area. Salinity intrusion length reaches 46 km along the Karun river, only 6 km behind the Darkhovin location. This distance needs about eight months to complete. The third scenario is based on a Karun freshwater discharge of 20 m^3/sec. According to the scenario results, saline water takes approximately 31 days to reach the barrage region. The saline water will travel roughly 32 km upstream along the Karun river, which will take around nine months to cover this distance. The fourth scenario is based on a freshwater discharge of 30 m^3/sec from the Karun river. According to the results of this scenario, saline water takes around two months to reach the barrage region. The saline water will travel around 18 km upstream along the Karun river, taking approximately eleven months to complete. The fifth scenario is based on a freshwater discharge from the Karun river of 40 m^3/sec. The findings of this scenario show that salty water takes around five months to reach the barrage location. At the end of the simulation period, the saline water will have traveled less than one kilometer along the Karun river. The sixth scenario is based on a freshwater discharge of 50 m^3/sec from the Karun river. According to the findings of this scenario, salty water travels around 68 kilometers and takes approximately four months to reach this place. The Karun river had no salty water flowing through it at the end of the simulation period. The seventh scenario is based on a freshwater discharge from the Karun river of 60 m^3/sec. This scenario's results indicate that salty water travels roughly 63 km and takes around five months to reach this location.

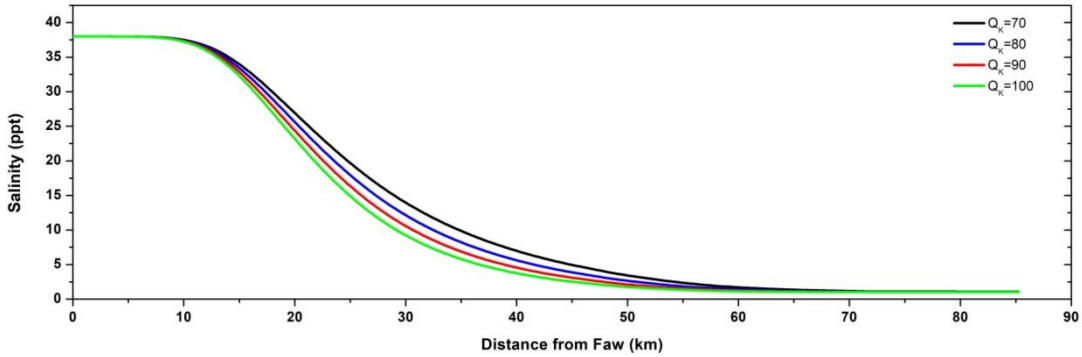

(Figure 6) Salinity intrusion length (km) along SARE corresponding to several freshwater inflow (70- 100 m^3/sec) from Karun River.

The remaining scenarios, namely the eighth, ninth, tenth, and eleventh, are based on freshwater discharges from the Karun river of 70, 80, 90, and 100 m3/sec, respectively. At the end of the simulation period, salty water travels about 58, 55, 51, and 47 km, respectively (figure 6).

Conclusions

The impact of a planned barrage on tidal hydrodynamics and salinity intrusion in the SARE was investigated using Mike11. The model's efficiency was evaluated by comparing model estimations to field observations of both water level and salinity. A reasonable agreement between the calculated and observed data was established. The calibrated model was then utilized to fulfill the study objectives.

However, the results indicated that the response of constituents amplitude to the presence of the barrage in the estuary system was spatially non-uniform, with substantial decreases and increases between different locations. The M2 amplitude shows a significant rise, notably around the barrage site, and a minor decrease in locations further distant from the barrage location. Similarly, the amplitudes of both S2 and N2 components increase significantly in places near the barrage site while decreasing somewhat in the other areas. Additionally, the amplitude of the principal diurnal constituents, K1 and O1 increases noticeably when the barrage is introduced to the estuary system. The response of the tidal components' phase shift to the barrage installation was additionally investigated. The results revealed that the most significant shifts occur between St2 and St1. The M2 phase shifts between St2 and St1 and reach 18 degrees, which means that a tidal wave will travel 37 minutes faster between these two locations. Similarly, for both S2 and N2, the most substantial changes in phase shifts occur between St1 and St2, with the phase change occurring at about 18 and 19 degrees, respectively. Furthermore, the phase difference between St1 and St2 for the diurnal components K1 and O1 will be reduced by around 12 degrees, implying that these tidal waves can depart St2 and arrive at St1 48 minutes earlier. Furthermore, the influence of the projected barrage on the tidal asymmetry is investigated. The results demonstrated that the relative phase relation remains less than 180 degrees, and the tidal asymmetry in SARE remains flood-dominant.

Additionally, a number of scenarios involving the freshwater inflow of the Karun River, ranging from 0 to 100 m^3/sec, were carried out to evaluate the response of salinity intrusion in the SARE to the barrage installation. The purpose was to identify the most suitable inflow to preserve the SARE environment from the salinity problem. Nevertheless, the results indicate that freshwater flows of 70, 80, 90, and 100 m^3/sec from the Karun river could be appropriate for maintaining the SARE environment, provided that the salinity incursion length does not exceed 60 km, which is considered a reasonable range in relation to the SARE hydrological state. The findings obtained above could be essential for many aspects of SARE management policy and may give vital insights to decision-makers.

Acknowledgment

The authors express their gratitude to DANIDA, the Danish International Development Agency, for providing them with the Mike 11 Software. The authors would also like to thank the technical teams from the Marine Science Center/ University of Basrah for their assistance in the field measurements.

References

Abdullah, S.S. 2002. Analysis of Tide Wave in Shatt Al-Arab Estuary, South of Iraq. Mesopotamian Journal of Marine Sciences, 17(2), 305-315.

Abdullah, A.D. 2016. Modelling Approaches to Understand Salinity Variations in a Highly Dynamic Tidal River: the case of the Shatt al-Arab River (1st ed.). CRC Press. https://doi.org/10.1201/9781315115948.

Abdullah, S. S.; Al-Fartousi, A. J. and Lafta, A. A., 2023. The impact of buildup proposed barrage on tidal hydrodynamics in the Shatt Al-Arab River, South of Iraq. Mesopotamian Journal of Marine Sciences, 38(1), 33–46. https://doi.org/10.58629/mjms.v38i1.325.

Ali, A.A. and Al-Thamiry, H.A., 2021. Controlling the salt wedge intrusion in Shatt Al-Arab River by a Barrage. Journal of Engineering, 27(12): 69-86. https://doi.org/10.31026/j.eng.2021.12.06.

Allafta, H. and Opp, C. 2020. Spatio-temporal variability and pollution sources identification of the surface sediments of Shatt Al-Arab River, Southern Iraq. scientific reports, 10 6979 pp. 1-16. https:// doi. org/10.1038/s41598-020-63893-w.

Al-Yamani, F. 2008. Importance of the freshwater influx from the Shatt-Al-Arab River on the Gulf marine environment. In: Abuzinada, A.H., Barth, HJ., Krupp, F., Böer, B., Al Abdessalaam, T.Z. (eds) Protecting the Gulf's Marine Ecosystems from Pollution. Birkhäuser Basel. https://doi.org/10.1007/978-3-7643-7947-6_11

Aubrey, D.G. and Speer, P.E. 1985. A study of non-linear tidal propagation in shallow inlet/estuarine systems. Part I: Observations. Estuarine, Coastal and Shelf Science, 21(2), 185–205, https://doi.org/10.1016/0272-7714(85)90096-4.

DHI, 2007. Mike 11 a modeling system for rivers and channels, DHI software user guide.

Fairley, I., Ahmadian, R., Falconer, R., Willis, M. and Masters, I. 2014. The effects of a Severn barrage on wave conditions in the Bristol channel. Renewable Energy, 68: 428-442. https://doi.org/10.1016/j.renene.2014.02.023.

Friedrichs, C.T. and Aubrey, D.G. 1988. Non-linear tidal distortion in shallow well-mixed estuaries: A synthesis. Estuarine, Coastal and Shelf Science, 27(5), 521–545, https://doi.org/10.1016/0272-7714(88)90082-0.

Guo, L. ; Wang, Z.B. ; Townend, I. and He, Q. 2019. Quantification of Tidal Asymmetry and Its Nonstationary Variations, Journal of Geophysics Research: Ocean, 124(1), 773–787. https://doi.org/10.1029/2018JC014372.

Haddout, S. and Maslouhi, A. 2018. One-Dimensional Hydraulic Analysis of the Effect of Sea Level Rise on Salinity Intrusion in the Sebou Estuary, Morocco. Marine Geodesy, 41, pp. 270–288. https:// doi. org/10.1080/01490419.2017.1420713.

Iglesias, I.; Ailez-Valente, P.; Bio, A. and Bastos, L. 2019. Modeling the main hydrodynamic pattern in shallow water estuaries: The Minho case study. Water, 1(5), 1040; https://doi.org/10.3390/w11051040.

Kuang, C.; Liang, H.; Mao, X.; Karney, B.; Gu, J.; Huang, H.; Chen, W. and Song, H. 2017. Influence of potential future sea-level rise on tides in the China sea. Journal of Coastal Research, 33 (1), 105–117. http://dx.doi.org/10.2112/JCOASTRES-D-16-00057.1.

Lafta, A.A.; Al-Taei, S.A. and Al-Hashimi, N.H., 2020. Impacts of Potential Sea-Level Rise on Tidal Dynamics in Khor Abdullah and Khor Al-Zubair, Northwest of Arabian Gulf . Earth System and Environment, 4 pp. 93–105. https:// doi. org/10.1007/s41748-020-00147-9.

Lafta, A.A. 2021. Estimation of Tidal excursion Length Along The Shatt Al-Arab Estuary, Southern Iraq. Vietnam Journal of Science and Technology, 59 (1). https:// doi. org/10.15625/2525-2518/59/1/15433.

Lafta, A.A. 2022. Investigation of tidal asymmetry in the Shatt Al-Arab river estuary, Northwest of Arabian Gulf. Oceanologia, 64, 376—386. https://doi.org/10.1016/j.oceano.2022.01.005.

Liu, W. and Liu, H. 2014. Assessing the Impacts of Sea Level Rise on Salinity Intrusion and Transport Time Scales in a Tidal Estuary, Taiwan. Water, 6, pp. 324–344. https:// doi. org/ 10.3390/w6020324.

Lu, S.; Tong, C.; Lee, D.Y.; Zheng, J.; Shen, J.; Zhang, W. and Yan, Y. 2015. Propagation of tidal waves up in Yangtze Estuary during the dry season. Journal of Geophysical Research: Oceans, 120 (9), 6445–6473, https://doi.org/10.1002/2014JC010414.

Mao, Q.; Shi, P.; Yin, K.; Gan, J. and Qi, Y. 2004. Tides and tidal currents in the Pearl River Estuary. Continental Shelf Research, 24: 1797–1808. https://doi: 10.1016/j.csr.2004.06.008.

Mahmood, A. B.; Abdullah, S. S. and Lafta, A. A. 2022. Proposed treatment to reduce salinity intrusion into the Shatt Al-Arab estuary by using temporary storage in a convergent of channel in the context of tide. International Journal of River Basin Management, DOI:10.1080/15715124.2022.2101466.

Moyel ,M.S. and Hussain, N.A. 2015. Water quality assessment of the Shatt al-Arab River, Southern Iraq. Journal of Coastal Life Medicine, 3(6) pp. 459-465. https:// doi. org/ 10.12980/JCLM.3.2015J5-26.

Neill, S.P.; Angeloudis, A.; Robins, P.E.; Walkington, I.; Ward, S.L.; Masters, I.; Lewis, M.J.; Piano, M.; Avdis, A.; Piggott, M.D.; Aggidis, G.; Evans, P.; Adcock, T.A.; Židonis, A.; Ahmadian, R. and Falconer, R. 2018. Tidal range energy resource and optimization-past perspectives and future challenges. Renew Energy, 127: 763-778. https://doi.org/10.1016/j.renene.2018.05.007.

Parsa, J.; Shahidi, E.A.; Hosseiny, S. and Yeganeh-Bakhtiary, A. 2007. Evaluation of computer and empirical models for prediction of salinity intrusion in the Bahmanshir estuary. Journal of Coastal Research, SI50 (Proceedings of the 9th International Coastal Symposium), 658 – 662. Gold Coast, Australia. https://www.jstor.org/stable/26481668.

Provost, L. C. 1991. Generation of overtides and compound tides (review). In B. B. Parker (Ed.), Tidal Hydrodynamics (pp. 269–295). Toronto: John Wiley.

Qian, M.; Tulio, M.M. and Thomas, A.A. 2019. The impact of a tidal barrage on coastal flooding due to storm surge in the Severn Estuary. Journal of Ocean Engineering and Marine Energy, 5: 217-226. http://dx.doi.org/10.1007/s40722-019-00143-w.

Shivaprasad, A.; Vinita, J.; Revichandran, C.; Manoj, N.T.; Srinivas, K.; Reny, P.D.; Ashwini, R. and Muraleedharan, K.R. 2013. Influence of saltwater barrage on tides, salinity, and

chlorophyll a in Cochin estuary, India. Journal of Coastal Research, 29 (6) pp. 1382–1390. https:// doi. org/ 10.2112/JCOASTRES-D-12-00067.1.

Siddig, N.A.; Al-Subhi A.M. and Alsaafani, M.A., 2019. Tide and mean sea level trend in the west coast of the Arabian Gulf from tide gauges and multi-missions satellite altimeter. Oceanologia, 61, 401–411. https://doi.org/10.1016/j.oceano.2019.05.003.

Song, D.; Wang, X.H.; Kiss, A.E. and Bao, X. 2011. The contribution to tidal asymmetry by different combinations of tidal constituents. Journal of Geophysical. Research, 116, C12007, https://doi:10.1029/2011JC007270.

Suh, S.W.; Lee, H.Y. and Kim, H.J. 2014. Spatio-temporal variability of tidal asymmetry due to multiple coastal constructions along the west coast of Korea. Estuaries. Coastal And Shelf Science, 151, 336-346. https://doi: 10.1016/j.ecss.2014.09.007.

Vinita, J.; Shivaprasad, A.; Manoj, N.T.; Revichandran, C.; Naveenkumar, K.R. and Jineesh,V K. 2015. Spatial tidal asymmetry of Cochin estuary, West Coast, India. Journal of Coastal Conservation, 19, 537–551. https://doi.org/10.1007/s11852-015-0405-9.

Wachler, B.; Seiffert, R.; Rasquin C. and Kösters, F. 2020. Tidal response to sea level rise and bathymetric changes in the German Wadden Sea. Ocean Dynamics, 70, 1033–1052. https:// doi. org/10.1007/s10236-020-01383-3.